Secondary defect formation in bonded silicon-on-insulator after boron implantation

A. F. Saavedra,[a] A. C. King, and K. S. Jones
Department of Materials Science and Engineering, SWAMP Center, University of Florida, Gainesville, Florida 32611

E. C. Jones
Department of Electrical and Computer Engineering, Oregon State University, Corvallis, Oregon 97331

K. K. Chan
IBM Semiconductor Research and Development Center, Research Division, Yorktown Heights, New York 10598

(Received 1 June 2003; accepted 17 November 2003; published 4 February 2004)

Silicon-on-insulator (SOI) has proven to be a viable alternative to traditional bulk silicon for fabrication of complementary metal–oxide–semiconductor devices. However, a number of unusual phenomena with regards to diffusion and segregation of dopants in SOI have yet to be explained. In the present study, SOITEC wafers were thinned to 700 and 1600 Å using oxidation and etching. Ion implantation was performed into SOI and bulk silicon wafers using $^{11}B^{+}$ ions at 6.5 and 19 keV with a dose of $3\times10^{14}\,cm^{-2}$. Thermal processing occurred in a furnace at 750 °C for times ranging from 5 min to 8 h under an inert ambient. Using quantitative transmission electron microscopy it was observed that the concentration of trapped interstitials and density of {311} defects was significantly reduced in SOI compared to the bulk. Hall effect was used to monitor the activation process of boron in SOI and bulk silicon. Significantly less activation was observed in SOI compared to the bulk and was dependent on the surface silicon thickness. For the first time, a decrease in the trapped interstitial concentration is observed in SOI even with minimal dose loss to the buried oxide. It is hypothesized that the formation of boron–interstitial clusters may be more pronounced in SOI, leading to a reduction in the trapped interstitial population and {311} defect density. [DOI: 10.1116/1.1640656]

I. INTRODUCTION

The advantages of silicon-on-insulator (SOI) over bulk silicon for the fabrication of future complementary metal–oxide–semiconductor (CMOS) integrated circuits have been well documented.[1,2] Some of these include reduced parasitic capacitance, elimination of latchup, increased speed, enhanced radiation hardness, and reduced power consumption. Despite these advantages, there are still unanswered questions about how scaling of the surface silicon layer could affect dopant diffusion and segregation around the surface Si/buried oxide (BOX) interface.

Damage from ion implantation often results in the formation of extended defects and other interstitial clusters upon thermal processing. This can lead to the detrimental effect of transient enhanced diffusion (TED), which is a major problem for formation of ultrashallow junctions in bulk silicon.[3,4] Thus, it becomes important to understand the role the surface silicon/BOX interface plays in interstitial recombination, as well as segregation of dopants in the proximity of the interface.

It has been known for years that certain dopants prefer to reside in silicon dioxide, while others prefer silicon.[5–9] Irregular diffusion in SOI materials has been investigated previously,[10–14] but there is still debate over its significance with regards to scaling of SOI devices. Some previous work has suggested that the surface silicon/BOX interface may not play a significant role in diffusion and segregation if the ion profile is a few hundred angstroms from the interface.[12,15] On the contrary, for profiles that are truncated by the interface, significant segregation and interstitial recombination have been shown to occur.[10,15] The current study set out to understand more about how secondary defect evolution differs in boron doped SOI compared to bulk silicon. Hopefully, this will shed light into both the recombination and segregation phenomena, which will become important for doping of future SOI devices.

II. EXPERIMENT

200 mm, *p*-type, {001}, 14–22 Ω cm, 4000 Å buried oxide UNIBOND® and 200 mm, *p*-type, {001}, 9–18 Ω cm bulk silicon wafers were used in the experiment. SOI wafers were thinned from an initial surface silicon thickness of 1600–700 Å using thermal oxidation in wet O_2, followed by etching in dilute HF (10:1). This yielded two SOI thicknesses (700 and 1600 Å) for comparison with the bulk silicon control. Thin screen oxides (20 Å) were deposited using low pressure chemical vapor deposition (LPCVD) to reduce channeling of the implanted ions. Wafers were then implanted with nonamorphizing, $^{11}B^{+}$, 6.5 and 19 keV, $3\times10^{14}\,cm^{-2}$ ions at room temperature with 7° tilt and 22° twist angles. A 200 Å low temperature oxide (LTO) cap oxide was deposited via chemical vapor deposition (CVD) in order to prevent out-

[a]Electronic mail: asaav@ufl.edu

diffusion of the boron during thermal processing. Samples were heated in a Thermolyne quartz tube furnace at 750 °C for times ranging from 5 min to 8 h under a nitrogen ambient.

Standard preparation techniques were used to make plan-view transmission electron microscopy (PTEM) samples. These included cutting a 3-mm-diam disk, followed by grinding using a 15 μm alumina slurry. Chemical etching was done using a solution of HF:HNO_3 (1:3) until a hole was made. A buffered oxide etch (BOE) 6:1 for approximately 3–5 min was necessary in order to assist in removal the buried oxide following etching in HF:HNO_3. A JEOL 200CX TEM, operating at 200 kV, was used to image the PTEM specimens under **g**(3**g**) weak-beam dark-field (WBDF) conditions. Quantitative TEM (QTEM) was used to calculate the trapped interstitials in extended defects and interstitial clusters, as well as the defect density and defect size.

Hall effect was performed at room temperature using an MMR Technologies model MPS-50 programmable power supply with a H-50 Hall, van der Pauw controller. Samples were cut into a square van der Pauw geometry with edge lengths between 1 and 1.4 cm and Ohmic contacts were made using 99.99 wet % indium. Current was varied from 1 μA to 1 mA in order to check the linearity of the measured values. A magnetic field of $\pm$3000 G was used in all of the measurements.

III. RESULTS

It should be understood that a certain amount of dose and interstitials are lost to the BOX when the implant profile overlaps with the interface. This overlap becomes increasingly important as the implant energy is increased and/or the surface silicon layer thinned. Ion profiles were simulated using UT-Marlowe in order to approximate the retained dose within the surface silicon layer of the SOI.[16] Significant overlap occurs for both implant energies in the 700 Å SOI. The 700 Å SOI loses approximately 6% of the dose at 6.5 keV and more than 50% at 19 keV. The 1600 Å retains the entire dose at 6.5 keV and loses 3% at 19 keV.

PTEM micrographs for the 6.5 keV implant energy are shown in Fig. 1, illustrating the extended defect evolution process in SOI and bulk. In the bulk silicon, an assortment of {311} and dot defects can be seen after both 15 and 30 min of annealing. However, in the SOI only dot defects appear. A significant difference, not only in the defect structure, but also in the size and density can be seen. The dot defects in the 700 Å SOI are much smaller than those in the 1600 Å and have nearly dissolved after annealing for 30 min. After annealing for 60 min, the defects in the 700 Å can no longer be resolved due to the QTEM detection limit of 6 $\times 10^9\,\mathrm{cm}^{-2}$; they are assumed to have dissolved at this point. The defects in the 1600 Å and bulk dissolve after annealing between 1 and 2 h. The QTEM data for the 6.5 keV specimens is shown in Fig. 2. It shows the concentration of interstitials trapped in extended defects as a function of the annealing time at 750 °C. This is partly explained by the truncation of the implant profile by the surface silicon/BOX interface. In the 1600 Å, there appears to be a reduction in Si_I ($\sim$50%) after annealing 30 min, but no enhancement in the decay rate compared to the bulk silicon. Figure 3 shows the active dose measured using Hall effect as a function of the anneal time. A reduction in the active dose can clearly be seen between the SOI and bulk silicon. This is not surprising for the 700 Å SOI due to the 6% dose loss of part of the implanted profile to the BOX. However, the 1600 Å did not suffer any dose loss at this energy and may be expected to be similar to the bulk in terms of activation; this is clearly not the case. A 70%–80% decrease in the active dose is obtained for the 700 Å SOI, as well as a $\sim$60% decrease in the 1600 Å. These differences between SOI and bulk silicon are discussed further in the discussion section.

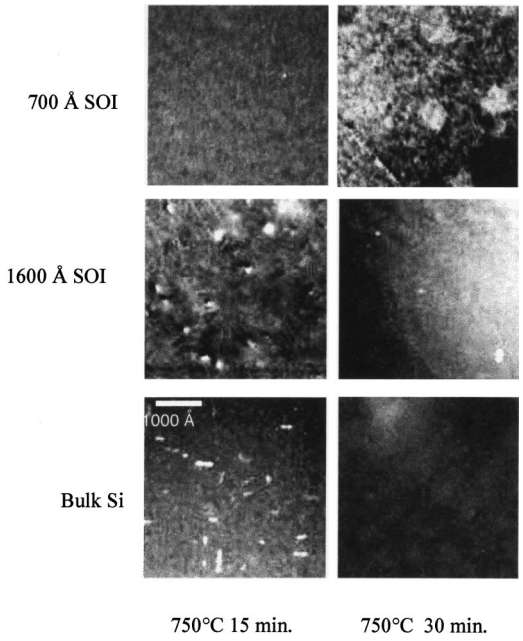

FIG. 1. PTEM WBDF micrographs of defect evolution in SOI and bulk for B^+, 6.5 keV, $3\times10^{14}\,\mathrm{cm}^{-2}$.

Figure 4 shows some of the PTEM micrographs for the 1600 Å and bulk implanted at 19 keV. The 700 Å SOI does not form extended defects, which is partly attributed to the

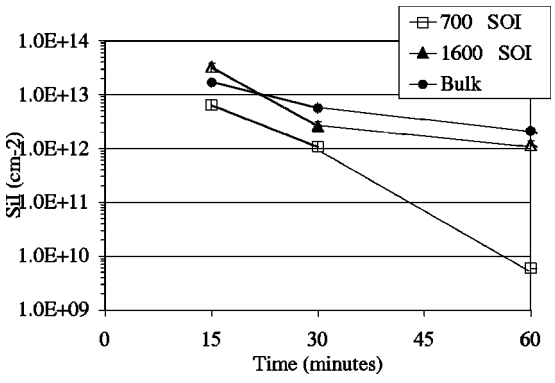

FIG. 2. Trapped interstitial concentration (Si_I) as a function of annealing time for B^+, 6.5 keV, $3\times10^{14}\,\mathrm{cm}^{-2}$ specimens.

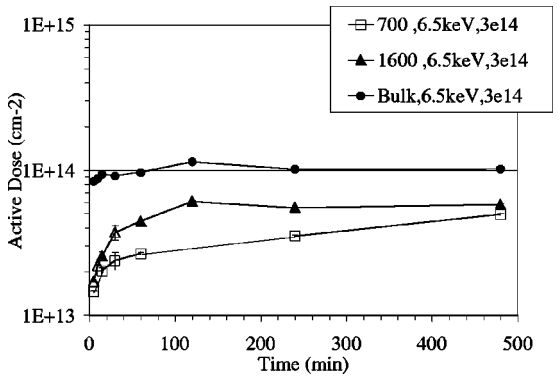

FIG. 3. Active dose of boron with annealing time for B^+, 6.5 keV, $3\times10^{14}\,cm^{-2}$ specimens measured using Hall effect.

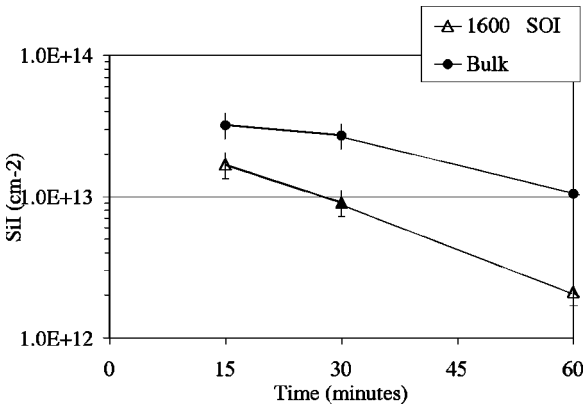

FIG. 5. Concentration of trapped interstitials as a function of time for B^+, 19 keV, $3\times10^{14}\,cm^{-2}$ specimens.

large dose loss (>50%) of the implanted profile. Thus, no QTEM data can be obtained for the 700 Å. The 1600 Å shows an assortment of small dot defects, while the bulk silicon shows elongated {311} defects. These {311} can be seen to coarsen in the bulk silicon, while the dot defects in the 1600 Å have nearly dissolved after 30 min. The concentration of trapped interstitials for the 19 keV specimens is shown in Fig. 5. The 1600 Å loses 3% of the dose initially, but a 50% decrease in the initial value of Si_I is observed. There is also an enhancement of approximately 2× in the decay rate in the 1600 Å compared to the bulk silicon. After annealing for 2 h, the 1600 Å Si_I decays to the detection limit. Figure 6 shows the activation of the 19 keV, 700 Å, 1600 Å, and bulk specimens. Once again, the SOI shows significantly less activation compared to the bulk silicon despite only a 3% dose loss for the 1600 Å SOI. The 1600 Å SOI also has about a 50% less active dose than the bulk silicon, while the 700 Å has about 60%–70% less active dose than bulk silicon.

IV. DISCUSSION

Obviously, there is significant difference between SOI and the bulk, both in terms of defect microstructure and electrical activation. When compared to a similar previous experiment involving Si^+ implantation into SOI,[15] a significant difference in extended defect evolution is obtained by using a nonisovalent species such as boron. In that experiment, no difference in Si_I or the defect microstructure was observed between SOI and bulk silicon as long as less than 6% dose loss occurred. However, in the present study a significant difference in Si_I is observed between SOI and the bulk for dose losses much less than 6%. Saavedra *et al.*,[15] also did not observe any enhancement in the decay rate until after 14% dose loss. An enhanced decay rate is observed for as low as a 3% dose loss in the 1600 Å SOI at 19 keV. The reason for the reduction in Si_I for low dose losses most obviously may be attributed to segregation of boron towards the surface Si/BOX interface. If a boron–interstitial pair was easily able to diffuse towards the surface Si/BOX interface, it may explain why fewer trapped interstitials were observed in SOI. However, no segregation was observed in secondary ion mass spectrometry (SIMS) data performed on the 1600 Å SOI, 19 keV, $3\times10^{14}\,cm^{-2}$ after annealing for 30 min at 750 °C. Instead, the boron profiles showed no difference between the 1600 Å SOI and bulk until the BOX was reached. Another hypothesis may then be proposed. This may be an enhance-

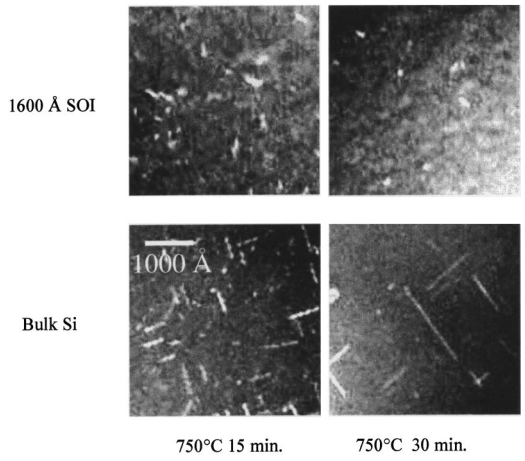

FIG. 4. PTEM WBDF micrographs of defect evolution in SOI and bulk for B^+, 19 keV, $3\times10^{14}\,cm^{-2}$.

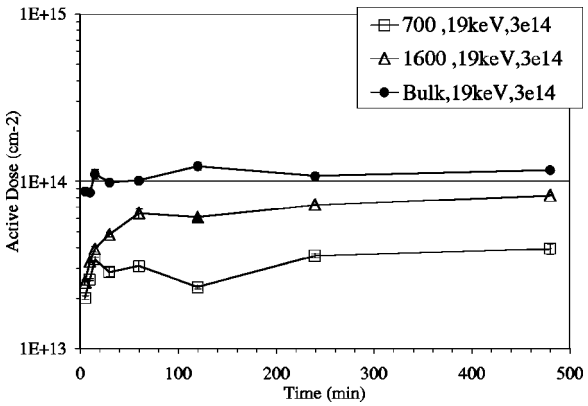

FIG. 6. Active dose of boron with annealing time for B^+, 19 keV, $3\times10^{14}\,cm^{-2}$ specimens measured using Hall effect. Error bars are smaller than the symbol size.

ment in the formation of boron–interstitial clusters (BICs) in SOI compared to bulk silicon. This could explain the decrease in the trapped interstitial populations observed in the SOI, since the BICs are submicroscopic. At the implanted dose of $3\times10^{14}\,\mathrm{cm}^{-2}$, the threshold for clustering of boron ($1\times10^{19}\,\mathrm{cm}^{-2}$) is well exceeded. However, at this point it would be premature to speculate on the source or mechanism causing this to occur within the surface silicon layer.

The electrical data also show differences between SOI and bulk, contrary to previous experiments in As^+ implanted SIMOX material.[17] Regardless of surface silicon thickness, a decrease in active dose is observed in SOI. An enhancement in the BIC population could explain why the boron is not being electrically activated to the extent of bulk silicon. A significant difference in hole mobility between the SOI (50–86 $\mathrm{cm}^2/\mathrm{V\,s}$) and the bulk (300–350 $\mathrm{cm}^2/\mathrm{V\,s}$) also supports the BIC theory, since BICs could possibly act as scattering sites in the silicon lattice. Both the reduced activation and hole mobility influence the sheet resistance. The measured increase in sheet resistance ranges from 10× to 26× for the 700 Å SOI, and from 7× to 12× for the 1600 Å SOI. The mobility decrease may also be due to an increase in the number of trapping impurities (e.g., C or O) in the surface silicon layer of the UNIBOND® material compared to the bulk. It should be mentioned that the reduction in Si_I closely parallels that of the reduction in active dose for the 700 and 1600 Å SOI. This may indicate that the interstitials not trapped by the {311} and dot defects in SOI may be participating in BIC formation, thus reducing the active dose of boron.

V. CONCLUSIONS

Secondary defect evolution and electrical activation after B^+ implantation have been studied in SOITEC SOI material and bulk silicon. Discrete differences in defect microstructure are observed between 1600 Å SOI and the bulk despite complete confinement of the implant profile within the surface silicon layer. For the first time, a decrease in the trapped interstitial concentration is observed in SOI even with minimal dose loss to the buried oxide. Enhancements in the decay rate of the trapped interstitial population are also observed at lower than expected dose losses. Reductions in both active dose and mobility may indicate an enhancement in the formation of boron–interstitial clusters in SOI compared to bulk silicon. Future experiments will focus on the source of the reduction in Si_I, including the role other impurities could play in the BIC formation process in SOI.

ACKNOWLEDGMENTS

The work of the Advanced Silicon Technology Laboratory (ASTL) at the IBM T.J. Watson Research Center was greatly appreciated. Mikhail Klimov of the University of Central Florida provided SIMS analysis for many of the SOI samples. Collaborations with Omer Dokumaci of IBM and Susan Earles of the Florida Institute of Technology were also critical to the design of the experiment. This research was sponsored by the Semiconductor Research Corporation (SRC) under Task No. 819.001.

[1] J. P. Colinge, *Silicon-on-Insulator Technology: Materials to VLSI*, 2nd ed. (Kluwer Academic, Boston, MA, 1997), pp. 1–4.
[2] A. O. Adan, T. Naka, A. Kagisawa, and H. Shimizu, Proceedings of the IEEE International SOI Conference (1998), p. 8.
[3] E. C. Jones and E. Ishida, Mater. Sci. Eng., R. **24**, 1 (1998).
[4] E. Chason, S. T. Picraux, J. M. Poate, J. O. Borland, M. I. Current, T. Diaz De la Rubia, D. J. Eaglesham, O. W. Holland, M. E. Law, C. W. Magee, J. W. Mayer, J. Melngailis, and A. F. Tasch, J. Appl. Phys. **81**, 6513 (1997).
[5] A. S. Grove, O. Leistiko, and C. T. Sah, J. Appl. Phys. **35**, 2695 (1964).
[6] F. Iacona, V. Raineri, and F. La Via, Phys. Rev. B **58**, 10990 (1998).
[7] S. A. Schwarz, R. W. Barton, C. P. Ho, and C. R. Helms, J. Electrochem. Soc. **128**, 1101 (1981).
[8] J. S. Williams, M. Petravic, Y. H. Li, J. A. Davies, and G. R. Palmer, Nucl. Instrum. Methods Phys. Res. B **64**, 156 (1992).
[9] G. A. Sai-Halasz, K. T. Short, and J. S. Williams, IEEE Electron Device Lett. **6**, 285 (1985).
[10] H. Park, E. C. Jones, P. Ronsheim, C. Cabral, Jr., C. D'Emic, G. M. Cohen, R. Young, and W. Rausch, Tech. Dig. - Int. Electron Devices Meet. 1999, p. 337.
[11] H. Uchida, Y. Ieki, M. Ichimura, and E. Arai, Jpn. J. Appl. Phys., Part 2 **39**, L137 (2000).
[12] O. Dokumaci, P. Ronsheim, A. Ajmera, J. Mayo, R. Young, C. Heenan, D. Uriarte, K. P. Muller, and R. J. Miller, presented at the MRS Spring Meeting, Symposium C, San Francisco, CA (2002).
[13] C. Y. Wong, C. R. M. Grovenor, P. E. Batson, and R. D. Isaac, J. Appl. Phys. **58**, 1259 (1985).
[14] P. Normand, D. Tsoukalas, N. Guillemot, and P. Chenevier, J. Appl. Phys. **66**, 3585 (1989).
[15] A. F. Saavedra, J. Frazer, K. S. Jones, I. Avci, S. K. Earles, M. E. Law, and E. C. Jones, J. Vac. Sci. Technol. B **20**, 2243 (2002).
[16] UT-Marlowe Version 5.0.
[17] A. K. Robinson, K. J. Reeson, and P. L. F. Hemment, J. Appl. Phys. **68**, 4340 (1990).